Surface Density Determination in Membranes by Fluorescence Energy Transfer†

Bernard Kwok-Keung Fung and Lubert Stryer*

ABSTRACT: Energy transfer between fluorescent-labeled phospholipids in synthetic membrane vesicles was investigated to ascertain the dependence of the transfer efficiency on the surface density of the energy acceptor in a random array. The fluorescent phospholipids used in this study were 1,5-dansylphosphatidylethanolamine (1,5-DPE), 2,6-dansylphosphatidylethanolamine (2,6-DPE), 2,5-dansylphosphatidylethanolamine (2,5-DPE), and eosinphosphatidylethanolamine (EPE). The fluorescent probes were incorporated into single bilayer vesicles formed from phosphatidylcholine. The surface densities of energy acceptor resulting in 50% transfer were 0.0066, 0.0057, 0.01, and 0.024 acceptors per phospholipid for transfer from 1,5-DPE to EPE, 2,5-DPE to EPE, 2,6-DPE to EPE, and 2,6-DPE to 2,5-DPE, respectively. The observed dependence of transfer efficiency on surface density of the acceptor was in good agreement with that calculated for a random planar distribution according to Förster's theory. The R_0 values derived from the observed transfer efficiencies are 46, 49, 38, and 26 Å for these donor–acceptors, which agree well with the values of 49, 51, 39, and 23 Å, respectively, calculated from their spectroscopic properties. In addition, the nanosecond emission kinetics of 2,6-DPE in the presence of several surface densities of EPE agree well with the theoretical prediction. These experiments show that energy transfer spectroscopy can provide quantitative information about the surface densities of chromophores in membranes and suggest that this technique should be valuable in elucidating the lateral distribution of labeled lipids and proteins.

Fluorescence energy transfer has been used as a spectroscopic ruler in the 15–75 Å range in a wide variety of biological macromolecules and assemblies (for a review, see Stryer, 1978). In particular, lateral interactions of peptides and proteins in membranes have recently been investigated by this technique (Fernandez & Berlin, 1976; Veatch & Stryer, 1977; Vanderkooi et al., 1977). The dependence of the efficiency of energy transfer from gramicidin labeled with a fluorescent donor to gramicidin labeled with an energy acceptor showed that the gramicidin A transmembrane channel consists of two polypeptide chains (Veatch & Stryer, 1977). A similar approach was used to investigate the association of Ca^{2+}-ATPase in reconstituted membrane vesicles (Vanderkooi et al., 1977). The efficiency of energy transfer between donor-labeled and acceptor-labeled ATPase molecules was found to be unaffected by a tenfold dilution of the lipid phase with phosphatidylcholine, whereas it was abolished by the addition of excess unlabeled ATPase, suggesting that this active transport system is oligomeric in the membrane. In all these studies energy transfer between unassociated gramicidins or ATPases that may complicate the accurate measurements of transfer between chromophores within the oligomers was largely avoided by keeping the surface density of the donors and acceptors relatively low (e.g., 1 gramicidin per 1000 phospholipids). These studies thus raise the following question: What is the dependence of the transfer efficiency on the surface density of *unassociated* donors and acceptors? This information is needed to design and interpret energy transfer experiments in native membranes having a high surface density of a particular protein (e.g., rhodopsin in retinal disc membranes). In these systems, energy transfer between unassociated proteins may be appreciable. An additional motivation is the prospect of using energy transfer to investigate phase separations (Shimshick & McConnell, 1973; Kleemann & McConnell, 1974) and other changes in the lateral distributions of membrane lipids and proteins (Nicolson, 1976) accompanying membrane processes such as fusion (Pagano & Weinstein, 1978).

We report here quantitative studies of energy transfer between fluorescent-labeled phospholipids in synthetic membrane vesicles. Our choices of donors and acceptors were guided by several considerations. First, they should be good analogues of membrane lipids so that they are randomly distributed in the plane of the membrane. Second, the donor and acceptor chromophores should be located in the same transverse region of the membrane (e.g., the head group region) so that the distance between them is mainly lateral rather than transverse. Localization of the chromophores in the head group region would also minimize transfer from one leaflet of the bilayer to the other. Third, the donor–acceptor pairs should have a wide range of R_0 values. The fluorescent phospholipids synthesized to meet these criteria were three dansyl derivatives and an eosin derivative of phosphatidylethanolamine. These compounds give four donor–acceptor pairs with R_0 values ranging from 23 to 51 Å. We have found that the observed transfer efficiencies agree well with the values calculated for random arrays of acceptors in membranes using Förster's theory. These experiments indicate that the surface density of randomly distributed membrane components containing a chromophore can be accurately determined by energy transfer spectroscopy.

Theory

The kinetics and efficiency of energy transfer between donors and acceptors randomly distributed in two dimensions can be calculated using similar formulas derived by Förster (1949) for transfer in three dimensions. The rate of energy transfer k_T between a donor and an acceptor separated by a distance r is

$$k_T = (1/\tau_0)(R_0/r)^6 \quad (1)$$

† From the Department of Structural Biology, Sherman Fairchild Center, Stanford University School of Medicine, Stanford, California 94305. *Received July 20, 1978.* This work was supported by research grants from the National Institutes of Health (GM-24032 and EY-02005) and by a grant from the Jane Coffin Childs Memorial Fund for Medical Research to B.K.-K.F. Bernard K.-K. Fung is a fellow of the Jane Coffin Childs Memorial Fund for Medical Research. A preliminary account of this work was presented at the 1978 Biophysical Society Meeting.

0006-2960/78/0417-5241$01.00/0

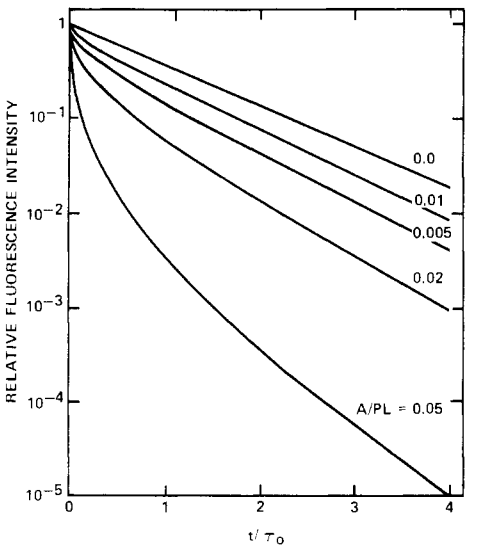

FIGURE 1: Calculated fluorescence emission kinetics of an energy donor in the presence of 0, 0.005, 0.01, 0.02, and 0.05 energy acceptors per phospholipid molecule. The lifetime of the donor in the absence of acceptor is τ_0. These decay curves were calculated for a random planar distribution of acceptors according to eq 3 and 4.

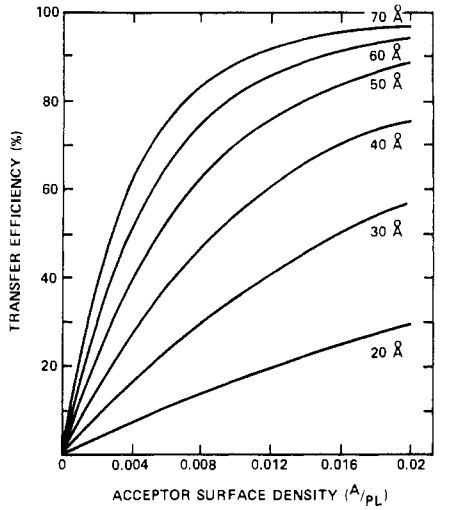

FIGURE 2: Calculated energy transfer efficiency as a function of the surface density of energy acceptor (acceptors per phospholipid) and the R_0 value for the donor-acceptor pair. These transfer efficiencies were calculated for a random planar distribution of acceptors according to eq 3-5.

where τ_0 is the excited state lifetime of the donor in the absence of acceptor. R_0, the distance (in Å) between the donor and acceptor at which the transfer efficiency is 50%, is given by

$$R_0 = (JK^2Q_0n^{-4})^{1/6} \times 9.79 \times 10^3 \quad (2)$$

where J is the spectral overlap integral (in $cm^3\ M^{-1}$), K^2 is the dipole-dipole orientation factor, Q_0 is the quantum yield of the donor in the absence of acceptor, and n is the refractive index of the medium. Consider a random planar array of donors and acceptors in which (1) there is no transfer between energy donors, (2) the number of acceptors in the excited state is small compared with the number in the ground state, (3) the distance between donors and acceptors does not change during the excited state lifetime of the donor, and (4) R_0 is the same for all donor-acceptor pairs. Under these conditions, the rate of transfer is the sum of k_T for all donor-acceptor pairs. The fluorescence intensity $F(t)$ of the donor in an infinite plane at time t following a very short light flash is then given by

$$F(t) = F(0)e^{-t/\tau_0}e^{-\sigma S(t)} \quad (3)$$

$$S(t) = \int_a^\infty [1 - e^{-(t/\tau_0)(R_0/r)^6}]2\pi r\mathrm{d}r \quad (4)$$

where $e^{-\sigma S(t)}$ is the energy transfer term, $F(0)$ is the initial fluorescence intensity, σ is the surface density of energy acceptors, and a is the distance of closest approach of donor and acceptor. These equations are essentially similar to those derived previously (Förster, 1949), except that $2\pi r\mathrm{d}r$, which is proportional to the probability of finding an acceptor within a distance r from the donor, replaces $4\pi r^2\mathrm{d}r$, the corresponding distribution element in three dimensions. Finally, the efficiency of energy transfer is given by

$$E = 1 - (1/\tau_0)\int_0^\infty F(t)/F(0)\mathrm{d}t \quad (5)$$

The preceding equations show that the fluorescence kinetics of the donor expressed as a function of t/τ_0, and the efficiency of energy transfer between donors and acceptors randomly distributed in a plane, depend only on three variables: R_0, σ, and a. In particular, the transfer efficiency is independent of the surface density of the donor. Donor fluorescence decay curves calculated by numerical integration of equations 3 and 4 for $R_0 = 40$ Å and σ ranging from 0 to 0.05 energy acceptors per phospholipid are shown in Figure 1. The area occupied by a phospholipid molecule is taken to be 70 $Å^2$ and so the closest approach distance is assumed to be $(70)^{1/2} = 8.4$ Å. As the surface density of energy acceptor increases, the average lifetime of the donor decreases and its emission kinetics deviate increasingly from a single exponential decay because of increasing energy transfer. The emission kinetics of a particular energy donor is monoexponential but that of the ensemble is not because the donors do not have identical arrays of acceptors surrounding them. The dependence of the transfer efficiency on the surface density of acceptor for R_0 values ranging from 20 to 70 Å is shown in Figure 2. For $\sigma = 0.01$ acceptor/phospholipid, the transfer efficiency varies from 18% for $R_0 = 20$ Å to 87% for $R_0 = 70$ Å. It is evident from Figure 2 that surface densities as low as 1 acceptor per 500 phospholipids (1 acceptor per 35 000 $Å^2$) result in appreciable energy transfer if the R_0 is larger than 30 Å. The choice of a is not critical provided that a is much smaller than R_0. Nearly the same transfer efficiencies are obtained for a ranging from 5 to 12 Å. The effects of energy transfer to acceptors in the opposite leaflet of a bilayer and of curvature are shown in the Appendix to be relatively small.

Experimental Procedures

Eosin 5-isothiocyanate, 1-dimethylaminonaphthalene-5-sulfonyl chloride, 2-dimethylaminonaphthalene-5-sulfonyl chloride, and 2-dimethylaminonaphthalene-6-sulfonyl chloride were purchased from Molecular Probes (Roseville, Minn.) and used without further purification. Thin-layer chromatography (TLC)[1] showed that their purity was higher than 95%. Egg yolk phosphatidylcholine (PC) was prepared by the method of Singleton et al. (1965). Phosphatidylethanolamine (PE) was purified from egg yolk lipid (Singleton et al., 1965) by silica

[1] Abbreviations used: TLC, thin-layer chromatography; PC, phosphatidylcholine; PE, phosphatidylethanolamine; 1,5-DPE, *N*-(1-dimethylaminonaphthalene-5-sulfonyl)phosphatidylethanolamine; 2,5-DPE, *N*-(2-dimethylaminonaphthalene-5-sulfonyl)phosphatidylethanolamine; 2,6-DPE, *N*-(2-dimethylaminonaphthalene-6-sulfonyl)phosphatidylethanolamine; EPE, *N*-eosin-*N'*-phosphatidylethanolaminothiourea; $NaDodSO_4$, sodium dodecyl sulfate.

gel chromatography (Hanahan et al., 1958). Purified phospholipids were stored at −20 °C in chloroform under nitrogen. The concentration of phospholipids was determined by phosphate assay (Chen et al., 1956).

The fluorescent-labeled phospholipids used in this study were synthesized by reacting the amino group of PE with eosin isothiocyanate or one of the isomers of dansyl chloride. *N*-(1-Dimethylaminonaphthalene-5-sulfonyl)phosphatidylethanolamine (1,5-DPE) and the 2,5 and 2,6 isomers of this compound (2,5-DPE and 2,6-DPE) were synthesized according to the procedure of Waggoner & Stryer (1970). Each of the purified products gave a single fluorescent spot (R_f about 0.7) on a silica gel TLC plate when developed with chloroform–methanol–water, 65:25:4. *N*-Eosin-*N'*-phosphatidylethanolaminothiourea (EPE) was synthesized by reacting 110 mg of eosin isothiocyanate with 100 mg of purified egg yolk PE in 1.5 mL of chloroform containing 0.1 mL of triethylamine. The reaction mixture was stirred gently for 1 h at room temperature and then examined by TLC as described above. Additional 5-mg portions of eosin isothiocyanate were added at 30-min intervals until there was no unreacted PE, as evidenced by the disappearance of the ninhydrin positive spot. The solvent was then removed under reduced pressure and the red solid material was redissolved in 1 mL of chloroform. This solution was then applied to several 20 × 20 cm preparative silica gel TLC plates that were previously activated by heating to 110 °C for 24 h. The plates were developed at room temperature in acetone–water 85:15. A small amount of unreacted eosin ran near the solvent front. The majority of EPE migrated as a broad band near the central region (R_f = 0.3–0.45), and a small amount of EPE trailed behind. After development, EPE from the major band was scraped off the plates, and eluted from the silica gel with chloroform–methanol (2:1). The EPE solution was taken to dryness in a nitrogen-purged rotary evaporator and redissolved in 1 mL of chloroform. The small amount of silica gel that precipitated out was removed by centrifugation. This procedure was repeated several times. The product gave a single spot by TLC in chloroform–methanol–water, 65:25:4 (R_f 0.65). Inorganic phosphate assay (Chen et al., 1956) gave 1 mol of phosphate per 8.5 × 10^4 OD units at 527 nm. EPE was stored at −20 °C in chloroform under nitrogen.

Preparation of Phospholipid Vesicles Containing Fluorescent Donor and Acceptor Probes. Single bilayer phospholipid vesicles containing donor–acceptor pairs of fluorescent-labeled PE were prepared by the ethanol injection procedure (Batzri & Korn, 1973). Aliquots of PC in chloroform were taken from a stock solution and the solvent was removed with a rotor evaporator under reduced pressure. The dry PC was redissolved in ethanol, and appropriate amounts of fluorescent donor and acceptor probes in ethanol were added. The concentration of phospholipid in this mixture was from 2 to 50 mM. A 0.25-mL aliquot of this ethanolic solution of PC and fluorescent-labeled PE was rapidly injected through a 30-gauge needle into 20 mL of 0.1 M sodium phosphate buffer, pH 7.2, under continuous and vigorous stirring. The size distribution of these phospholipid vesicles was measured by electron microscopy using negative-staining technique as previously described (Castle & Hubbell, 1976).

Fluorescence Measurements. Steady-state fluorescence emission and excitation spectra were obtained on a SPEX Fluorolog spectrofluorimeter operated in the E/R mode. This spectrofluorimeter gives corrected excitation spectra. Emission spectra were corrected for the wavelength dependence of the detection system as determined with a magnesium oxide scatterer and a calibrated photodiode (United Detector PIN 10-UV). The excitation and emission band widths are 4 nm. All spectra were measured at 22 °C. Fluorescence quantum yields were determined using 1-anilinonaphthalene-8-sulfonate in ethanol as a standard of quantum yield 0.37 (Stryer, 1965).

The peak absorbance of the samples in our fluorescence measurements was less than 0.1 to eliminate inner filter effects, except in one series of experiments requiring a higher donor concentration. In this case, a correction was made for the attenuation of the fluorescence intensity due to the inner filter effect. At the end of each measurement, an equal volume of 5% $NaDodSO_4$ in 0.05 M sodium phosphate buffer, pH 7.2, was added to solubilize all the phospholipid vesicles. The fluorescence intensities of the donors and acceptors at their emission maxima were measured again. The solubilization of the vesicles by detergent eliminated any energy transfer, thus making it feasible to accurately determine the concentration of donor and acceptor in each sample from their fluorescence intensities.

The fluorescence emission kinetics of the donor in the absence and presence of energy acceptor were measured with a single-photon counting nanosecond fluorimeter (Yguerabide et al., 1970; Yguerabide, 1972). Synchrotron radiation having a detected full width at half-maximum of 0.75 ns and a repetition rate of 1.28 MHz was used as the exciting light source (I. Munro, I. Pecht, & L. Stryer, submitted for publication). The band width of the 350 nm exciting light was 4 nm. The emission was passed through a 440-nm interference filter and detected by an RCA 8850 photomultiplier tube. The total fluorescence intensity $F(t)$ was taken to be $y(t) + 2x(t)$, where y and x were the vertically and horizontally polarized components of the emission when the sample was excited with vertically polarized light. The excited-state lifetime and rotational correlation time were determined by a nonlinear least-squares fit procedure which took into account the finite duration of the light pulse (Grinvald & Steinberg, 1974; Munro, Pecht, & Stryer, submitted for publication).

Results

Spectroscopic Characteristics of Fluorescent-Labeled Phospholipids in PC Vesicles. Single bilayer vesicles with an average diameter of 280 Å as shown by electron microscopy were formed by the ethanol injection method. Incorporation of up to 1 fluorescent phospholipid per 50 molecules of phosphatidylcholine did not appreciably change the distribution of vesicle sizes. The excitation and emission spectra of 2,6-DPE, 2,5-DPE, 1,5-DPE, and EPE in PC vesicles are shown in Figure 3. The absorption spectra of these probes are very similar to their excitation spectra. The emission spectra of 2,6-DPE, 1,5-DPE, and 2,5-DPE overlap to various extents the absorption spectra of EPE, thus providing a set of three donor–acceptor pairs with different R_0 values. In addition, there is a small overlap of the emission spectrum of 2,6-DPE and the absorption spectrum of 2,5-DPE, and so this pair was used to obtain a small R_0 distance. The donor quantum yields, spectral overlap integrals, and R_0 distances calculated from these parameters according to eq 2 using n = 1.4 and assuming $K^2 = 2/3$ are given in Table I.

Steady-State Fluorescence Measurements of Energy Transfer in PC Vesicles. The emission spectra of PC vesicles containing 2,6-DPE, the energy donor, and EPE, the energy acceptor, are shown in Figure 4. In this series of experiments, the surface density of energy acceptor was varied by changing the amount of PC while keeping that of 2,6-DPE and EPE constant. As the surface density of EPE increases, the 2,6-DPE fluorescence peaked at 435 nm decreases and the EPE fluo-

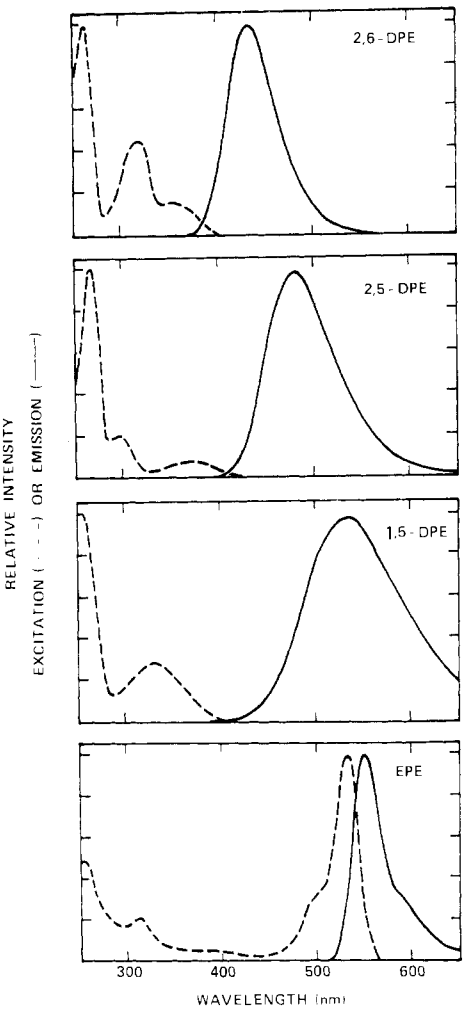

FIGURE 3: Excitation (- - -) and emission (—) spectra of fluorescent derivatives of PE in PC vesicles in 0.1 M sodium phosphate buffer, pH 7.2. The excitation and emission maxima of 2,6-DPE are 261 and 435 nm; 2,5-DPE, 266 and 480 nm; 1,5-DPE, 254 and 532 nm; and EPE, 532 and 550 nm, respectively. These spectra were obtained with vesicles containing 1 fluorescent chromophore per 200 molecules of PC. The molar extinction coefficients (cm^{-1} M^{-1}) are 5700 at 359 nm for 2,6-DPE, 3000 at 378 nm for 2,5-DPE, 4300 at 335 nm for 1,5-DPE, and 85 000 at 527 nm for EPE.

TABLE I: Comparison of Observed and Calculated R_0 Values.

donor	acceptor	Q_d	J (M^{-1} cm^3)	R_0(calcd) (Å)	R_0(obsd) (Å)
1,5-DPE	EPE	0.37	2.36×10^{-13}	48.7	46
2,5-DPE	EPE	0.76	1.54×10^{-13}	51.2	49
2,6-DPE	EPE	0.71	3.31×10^{-14}	39.1	37.5
2,6-DPE	2,5-DPE	0.71	1.3×10^{-15}	22.8	25.5

rescence peaked at 550 nm concomitantly increases because of energy transfer. At 430 nm, all of the emission comes from 2,6-DPE. Therefore the efficiency of energy transfer can be calculated from the quenching of the energy donor using

$$E = 1 - (F/F_0) \quad (6)$$

where F is the fluorescence intensity of 2,6-DPE at 430 nm in the presence of EPE and F_0 is the intensity in the absence of EPE. The transfer efficiency increases from 7 to 62% as the surface density of EPE increases from 0.001 to 0.016 per phospholipid.

The dependence of the transfer efficiency on the surface

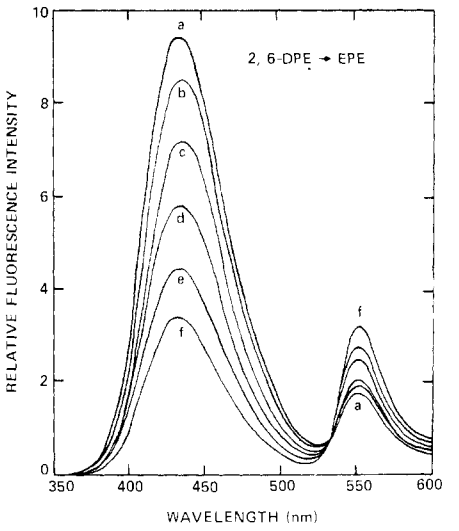

FIGURE 4: Emission spectra showing energy transfer from 2,6-DPE to EPE in phosphatidylcholine vesicles as a function of the ratio of PC to EPE: (a) 1000, (b) 540, (c) 215, (d) 110, (e) 80, and (f) 55. The molar ratio of 2,6-DPE to EPE was kept constant at 5:1. Samples containing 0.56 μM EPE were excited at 320 nm. The decrease in the emission intensity at 435 nm is accompanied by an increase at 550 nm due to energy transfer from 2,6-DPE to EPE.

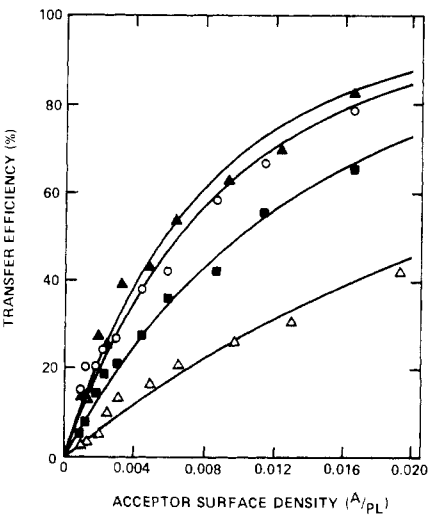

FIGURE 5: Energy transfer efficiency as a function of the surface density of energy acceptor (acceptors per phospholipid) for four donor–acceptor pairs in PC vesicles: 2,6-DPE to 2,5-DPE (△); 2,6-DPE to EPE (■); 1,5-DPE to EPE (○); and 2,5-DPE to EPE (▲). The best fit of these data to eq 3–5 (shown as solid curves) gives R_0 values of 25.5, 37.5, 49, and 46 Å, respectively. The molar ratio of donor to acceptor was kept constant in these experiments. The surface density of acceptor was varied by changing the amount of PC relative to that of acceptor and donor.

density of the energy acceptor was determined in this way for three other donor–acceptor pairs: 2,5-DPE to EPE; 1,5-DPE to EPE; and 2,6-DPE to 2,5-DPE. The fits of these observed transfer efficiencies to theoretical curves calculated from eq 3 are shown in Figure 5. The only adjustable parameter in these calculations was R_0. The best fits were obtained for R_0 values of 46, 49, 37.5, and 25.5 Å for transfer from 1,5-DPE to EPE, 2,5-DPE to EPE, 2,6-DPE to EPE, and 2,6-DPE to 2,5-DPE, respectively. As shown in Table I, these R_0 values are within 3 Å of those calculated from eq 2 for the observed donor quantum yields and spectral overlaps, assuming a refractive index of 1.4 and an orientation factor of 2/3. The assumption that K^2 approaches the value for a rapidly randomized en-

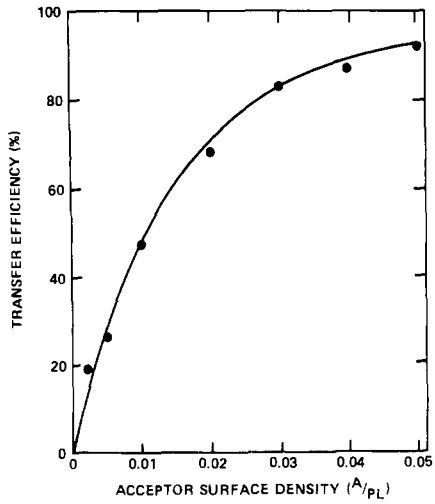

FIGURE 6: Energy transfer efficiency from 2,6-DPE to EPE as a function of the surface density of energy acceptor. The experimental points (●) determined from the decrease of the 2,6-DPE emission intensity at 430 nm on excitation at 320 nm best fit the curve (solid line) calculated from eq 3-5 for a R_0 of 36.5 Å. In these experiments, the ratio of 2,6-DPE to PC was kept constant. The surface density of the acceptor was varied by changing the amount of EPE relative to that of 2,6-DPE and PC.

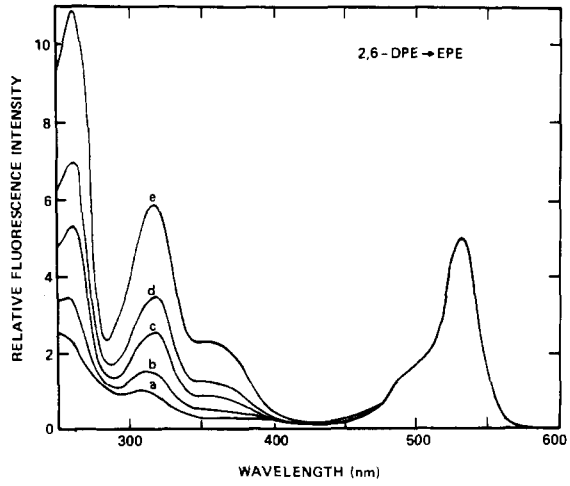

FIGURE 7: Excitation spectra of EPE, the energy acceptor, in PC vesicles in the presence of different amounts of 2,6-DPE, the energy donor. The concentration of EPE was 0.625 μM, and the molar ratio of PC to EPE was 100 in all samples. The molar ratio of 2,6-DPE to EPE was (a) 0, (b) 1, (c) 3, (d) 5, and (e) 10. The emission wavelength was 580 nm. All spectra were normalized to the same value at 532 nm.

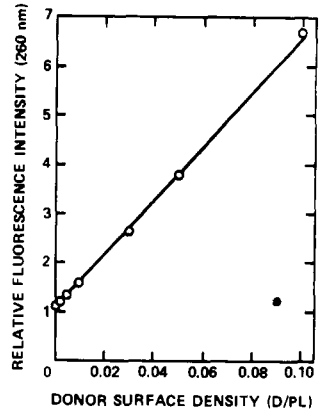

FIGURE 8: Relative intensity of EPE emission at 580 nm on excitation at 260 nm as a function of the surface density of 2,6-DPE, the energy donor. The open circles are intensities obtained from excitation spectra (as in Figure 7) and corrected for inner filter effects. The solid line is the least-squares fit.

semble is substantiated by nanosecond emission anisotropy measurements discussed below.

Energy transfer efficiencies were also measured for a series of vesicles containing a constant amount of 2,6-DPE and PC and differing amounts of EPE. Transfer efficiencies, determined from the quenching of the fluorescence of 2,6-DPE at 430 nm, ranged from 19 to 95% as the surface density of energy acceptor increased from 0.002 to 0.05 per phospholipid. As shown in Figure 6, these observed transfer efficiencies fit the theoretical curve calculated from eq 3 for R_0 = 36.5 Å, in good agreement with the value of 37.5 Å obtained experimentally by changing the amount of PC (described above) and the value of 39.5 Å calculated from spectroscopic parameters according to eq 2 (Table I).

The depencence of energy transfer efficiency on the surface density of energy donor can be determined from the excitation spectrum of the energy acceptor. The magnitude of the corrected excitation spectrum $G(\lambda)$ of the energy acceptor at excitation wavelength λ is given by

$$G(\lambda) = [\epsilon_a(\lambda)\sigma_a + E\epsilon_d(\lambda)\sigma_d]\gamma \quad (7)$$

where ϵ_a and ϵ_d are the extinction coefficients of the acceptor and donor, respectively, at wavelength λ, σ_a and σ_d are their surface densities, and γ is a constant which depends on the instrument and the energy acceptor. The excitation spectra of EPE, the energy acceptor, in the presence of increasing amounts of 2,6-DPE, the energy donor, are shown in Figure 7. The excitation spectrum in the absence of acceptor (curve a) is virtually identical with the absorption spectrum of EPE. As the surface density of 2,6-DPE increases, the excitation spectra of EPE (curves b-e) exhibit contributions peaked at 261, 320, and 358 nm arising from energy transfer. The magnitude of the excitation spectrum of EPE at 360 nm is plotted as a function of the surface density of 2,6-DPE in Figure 8. The linearity of this plot indicates that the efficiency of energy transfer is independent of the surface density of energy donor, as predicted by theory. The transfer efficiency calculated from the slope of this plot is 56%, in good agreement with the value of 50% obtained from the quenching of the donor fluorescence (Figure 5).

Nanosecond Fluorescence Measurements of Energy Transfer in PC Vesicles. The nanosecond emission kinetics of 2,6-DPE in PC vesicles containing various amounts of EPE is shown in Figure 9. The fluorescence kinetics of 2,6-DPE in the absence of EPE fits a single exponential decay with a lifetime of 13.2 ns. In the presence of increasing amounts of energy acceptor, the lifetime of 2,6-DPE becomes shorter and deviates increasingly from a single exponential decay (Figure 9), as predicted by theory. In Figure 9, the observed emission kinetics of 2,6-DPE are compared with the decay curves for different surface densities of energy acceptor calculated according to eq 3 and 4 and convoluted with the light pulse (solid lines in Figure 9). For these calculated curves, τ_0 = 13.2 ns (the observed value in the absence of EPE), and R_0 = 39.5 Å (the value calculated from spectroscopic parameters, as shown in Table I). It should be noted that no adjustable parameters were used in calculating these theoretical curves. The observed emission kinetics display less curvature than the theoretical curves. A possible reason for these differences is that there may be fewer donor-acceptor pairs at short distances than expected statistically because both the donor and acceptor are negatively charged.

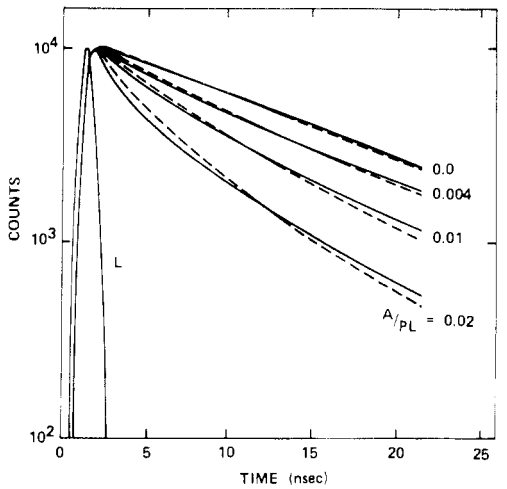

FIGURE 9: Fluorescence emission kinetics of 2,6-DPE in PC vesicles containing 0, 0.004, 0.01, and 0.02 molecules of EPE per molecule of PC (dashed lines). Synchrotron radiation was used as a pulsed light source. The excitation wavelength was 350 nm and the emission was viewed through a 440-nm interference filter. The excited state lifetime of 2,6-DPE in the absence of energy acceptor is 13.2 ns (solid line for $\sigma = 0$). The decay curves, calculated according to eq 3 and 4 for $R_0 = 39.5$ Å, $a = 8.4$ Å, and $\tau_0 = 13.2$ ns, and then convoluted with the light pulse, are shown as solid lines.

The nanosecond emission anisotropy kinetics of 2,6-DPE in PC vesicles were measured to determine the extent of rotational motion of this chromophore during its excited state lifetime and thereby place limits on the range of K^2. The observed emission anisotropy of 2,6-DPE in PC vesicles decreased linearly from a value of 0.164 at $t = 0$ (corresponding to the peak of the light pulse in Figure 9) to 0.02 at $t = 5$ ns. The rotational correlation time of 2.4 ns calculated from this very rapid depolarization indicates that the 2,6-DPE chromophore has a very large degree of rotational freedom during its excited state lifetime. If the chromophore of EPE has no rotational mobility and is oriented perpendicular to the line joining the donor and acceptor (the least favorable case), K^2 can assume a value between 0.33 and 1.33, which would give an apparent R_0 ranging from 0.89 to 1.12 times the actual R_0 (Stryer, 1978). Since EPE probably has a certain degree of rotational freedom, the range of uncertainty for R_0 should be even narrower.

Discussion

We have observed efficient energy transfer between fluorescent-labeled phospholipids in membrane vesicles containing 1 to 50 energy acceptors per 1000 phospholipids. The dependence of the transfer efficiency on the acceptor surface density in this range agrees closely with that predicted by theory for a random distribution of acceptors in two dimensions. The R_0 values derived from the observed transfer efficiency are 46, 49, 38, and 26 Å for the four donor-acceptor pairs, in good agreement with the R_0 values of 49, 51, 39, and 23 Å, respectively, calculated from their spectroscopic properties. Furthermore, the transfer efficiency was found to be independent of the concentration of donor, as expected from theory.

Our theoretical calculations of transfer efficiencies (Figure 2) were obtained by numerical integration of eq 3–5, which assume that the donor and acceptor are stationary during the excited state lifetime of the donor. The diffusion coefficients of phospholipids in fluid bilayers are approximately 10^{-8} cm^2/s (Scandella et al., 1972; Schlessinger et al., 1977). For $\tau_0 = 13.2$ ns (Figure 9), the mean distance diffused ($[4D\tau_0]^{1/2}$) during the lifetime of the donor is approximately 2 Å, which is small compared with the mean distance between the donor and acceptor (50–250 Å). A more exact calculation using the theory of Steinberg & Katchalski (1968) indicates that the increase in energy transfer efficiency due to diffusion is less than 1% under these conditions. It is of interest, however, to note that diffusion would markedly enhance transfer if a phospholipid containing a long-lived donor such as terbium ion, which has a lifetime in the millisecond range, were used (D. D. Thomas, W. F. Carlsen, & L. Stryer, submitted for publication). Surface densities as low as one acceptor per 10^5 phospholipids could then be measured.

TABLE II: Effect of Geometry on the Surface Density of Acceptor Resulting in 50% Energy Transfer σ_{50}(Acceptor/Phospholipid).[a]

R_0 (Å)	planar monolayer	planar bilayer	spherical monolayer	spherical bilayer
30	0.0160	0.0154	0.0162	0.0155
40	0.0087	0.0077	0.0087	0.0079
50	0.0055	0.0044	0.0055	0.0045
60	0.0038	0.0027	0.0038	0.0028
70	0.0028	0.0018	0.0028	0.0019

[a] In these calculations, $a = 8.4$ Å, $h = 50$ Å, $r_c = 140$ Å, and $r_i = 90$ Å. The chromophores in the spherical monolayer are assumed to be in the inner leaflet ($r_i = 90$ Å).

For the sake of simplicity, we compared our experimental results with those calculated for a random distribution of acceptors in a single infinite plane. The effects on transfer efficiency of having a bilayer instead of a monolayer and of having a spherical vesicle instead of a planar sheet of acceptors are considered in the Appendix. As shown in these calculations, the transfer efficiency in a spherical membrane (radius of 90 Å) is nearly the same as in a planar membrane, indicating that this degree of curvature has a negligible effect. For probes located at the surface of a bilayer membrane, there is little energy transfer from donors in one leaflet to acceptors in the opposite one, if the R_0 value is less than 40 Å. Energy transfer across the bilayer becomes significant for donors and acceptors located closer to the center of the bilayer or having a larger R_0 value (Table II). This effect, however, can readily be accounted for by the equations given in the Appendix, sections A and B.

The calculated dependence of the transfer efficiency on the surface density of acceptor and R_0 (Figure 2), as verified by our experimental measurements (Figure 5), provides criteria for designing experiments aimed at elucidating lateral interactions of membrane components in biological and reconstituted membranes. For example, in using energy transfer to determine whether a membrane protein is monomeric or oligomeric, transfer between unassociated donors and acceptors should be minimized. The curves shown in Figure 2 indicate that, for $R_0 = 30$ Å, the transfer efficiency between unassociated species is less than 10% when the surface density of energy acceptor is less than 0.003 per phospholipid. A higher observed transfer efficiency would reveal that the donor and acceptor are not randomly distributed throughout the membrane but rather are preferentially localized in a particular domain or are in fact associated. Furthermore, these curves are useful in choosing a donor-acceptor pair with an appropriate R_0 value for determining the absolute surface density of an energy acceptor.

Our present study suggests that energy transfer should be a valuable technique for accurately measuring the lateral distribution of proteins and phospholipids in membranes. For

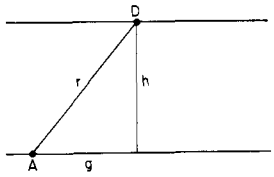

FIGURE 10: Energy transfer geometry in a planar bilayer.

example, the transfer efficiency between a donor attached to an unsaturated phospholipid and an acceptor attached to a saturated phospholipid would decrease markedly when these probes partition into different domains during a phase separation. Alternatively, the transfer efficiency would increase when labeled cell surface receptors are clustered by the binding of antibody. Moreover, the technique developed here should be useful for determining the extent of mixing of proteins and lipids in membrane fusion.

Acknowledgments

We thank Mr. Roger Koeppe II for assistance with computer programming and Dr. David D. Thomas for helpful discussions of theory.

Appendix

A. *Energy Transfer in an Infinite Planar Bilayer.* The kinetics and efficiency of energy transfer between donors and acceptors randomly distributed in a single infinite plane have been given in eq 3-5. We now consider energy transfer of a donor to acceptors randomly distributed in two infinite planes separated by a distance h, as in a planar bilayer membrane (Figure 10). The emission kinetics of the energy donor are given by

$$F(t) = F(0)e^{-t/\tau_0}e^{-\sigma[S_1(t)+S_2(t)]} \quad \text{(A1)}$$

where S_1, the quenching contribution arising from transfer between donors and acceptors in the same plane, is given by

$$S_1(t) = \int_a^\infty \left[1 - e^{-(t/\tau_0)(R_0/r)^6}\right] 2\pi r\,dr \quad \text{(A2)}$$

As in eq 4, a is the distance of closest approach of a donor and acceptor in the same plane, τ_0 is the lifetime of the donor in the absence of acceptor, R_0 is the critical distance at 50% transfer efficiency for a single donor-acceptor pair, and r is the distance between a donor and a particular acceptor. The expression for S_2, the quenching contribution arising from transfer between donors and acceptors in opposite planes, is derived by noting that the probability distribution for energy acceptors is $2\pi g\,dg$. Since $2\pi r\,dr = 2\pi g\,dg$, and $r = h$ for $g = 0$

$$S_2(t) = \int_h^\infty \left[1 - e^{-(t/\tau_0)(R_0/r)^6}\right] 2\pi r\,dr \quad \text{(A3)}$$

Equation A3 is essentially the same as that derived by Shaklai et al. (1977) in their studies of energy of transfer to hemoglobin bound to red cell membranes. Finally, the transfer efficiency is calculated by substituting $F(t)$ from eq A1 into eq 5.

B. *Energy Transfer in a Spherical Bilayer.* Consider a spherical bilayer in which the donors and acceptors are randomly distributed in an external shell of radius r_e and an internal shell of radius r_i (eq B1). The fraction f of donors in the external shell is assumed to be proportional to its relative area, and so $f = r_e^2/(r_e^2 + r_i^2)$. There are four energy transfer contributions: S_1, from transfer between donors and acceptors in the external shell; S_2, from transfer from donors in the external shell to acceptors in the internal shell; S_3, from transfer between donors and acceptors in the internal shell; and S_4, from transfer between donors in the internal shell and acceptors in the external shell. In this system, the emission kinetics of the donor are given by

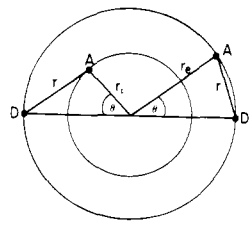

FIGURE 11: Energy transfer geometry in a spherical bilayer.

$$F(t) = F(0)e^{-t/\tau_0}[fe^{-\sigma[S_1(t)+S_2(t)]} + (1-f)e^{-\sigma[S_3(t)+S_4(t)]}] \quad \text{(B1)}$$

S_1, S_2, S_3, and S_4 are derived by expressing r in terms of θ (Figure 11). The probability distribution factor $2\pi r\,dr$ in eq A2 then becomes $2\pi r_e^2 \sin\theta\,d\theta$ for the outer shell and $2\pi r_i^2 \sin\theta\,d\theta$ for the inner shell of acceptors. The distance r between donors and acceptors in the outer shell is

$$r = [2r_e^2(1 - \cos\theta)]^{1/2} \quad \text{(B2)}$$

For the inner shell, r_i^2 replaces r_e^2 in the above expression. The distance between a donor in one shell and an acceptor in the other is given by

$$r = (r_e^2 + r_i^2 - 2r_e r_i \cos\theta)^{1/2} \quad \text{(B3)}$$

The lower limit of interaction θ_e for $S_1(t)$ is

$$\theta_e = \cos^{-1}\left(1 - \frac{a^2}{2r_e^2}\right) \quad \text{(B4)}$$

and for $S_3(t)$, the lower limit θ_i is

$$\theta_i = \cos^{-1}\left(1 - \frac{a^2}{2r_i^2}\right) \quad \text{(B5)}$$

where a is the distance of closest approach of the donor and acceptor. Substitution of these expressions gives

$$S_1(t) = \int_{\theta_e}^\pi \left[1 - e^{(-t/\tau_0)}\frac{R_0^6}{8r_e^6(1-\cos\theta)^3}\right] 2\pi r_e^2 \sin\theta d\theta \quad \text{(B6)}$$

$$S_2(t) = \int_0^\pi \left[1 - e^{-(t/\tau_0)}\frac{R_0^6}{(r_e^2 + r_i^2 - 2r_e r_i\cos\theta)^3}\right] \times 2\pi r_i^2 \sin\theta d\theta \quad \text{(B7)}$$

$$S_3(t) = \int_{\theta_i}^\pi \left[1 - e^{-(t/\tau_0)}\frac{R_0^6}{8r_i^6(1-\cos\theta)^3}\right] 2\pi r_i^2 \sin\theta d\theta \quad \text{(B8)}$$

$$S_4(t) = \int_0^\pi \left[1 - e^{-(t/\tau_0)}\frac{R_0^6}{(r_e^2 + r_i^2 - 2r_e r_i\cos\theta)^3}\right] \times 2\pi r_e^2 \sin\theta d\theta \quad \text{(B9)}$$

C. *Effect of Geometry on Energy Transfer.* The dependence of the transfer efficiency on R_0 and σ was calculated using the preceding equations for donors and acceptors arranged in a planar monolayer, a planar bilayer, a spherical monolayer, and a spherical bilayer. The surface densities (σ_{50}) of energy acceptor corresponding to 50% energy transfer in each of these arrays are given in Table II. The transfer efficiencies for the planar monolayer and the spherical monolayer are almost identical for all values of R_0 and σ showing that the curvature of even the inner leaflet of a small vesicle (r_i = 90 Å) has a

negligible effect on the transfer efficiency. The difference between a planar monolayer and planar bilayer is larger, especially for R_0 values larger than about 40 Å. This effect is expected, since energy transfer across the bilayer becomes more effective when the R_0 is comparable to or larger than the distance between the layers of donors and acceptors. For example, for R_0 = 50 Å, σ_{50} decreases from 0.055 for a planar monolayer to 0.044 acceptor per phospholipid for a planar bilayer. Again, there is little difference between the transfer efficiency in a planar bilayer and a spherical bilayer.

References

Batzri, S., & Korn, E. D. (1973) *Biochim. Biophys. Acta 298,* 1015.

Castle, J. D., & Hubbell, W. L. (1976) *Biochemistry 15,* 4818.

Chen, P. S., Toribara, T. Y., & Warner, H. (1956) *Anal. Chem. 28,* 1756.

Fernandez, S. M., & Berlin, R. D. (1976) *Nature (London) 264,* 411.

Förster, T. (1949) *Z. Naturforsch. 49,* 321.

Grinvald, A., & Steinberg, I. Z. (1974) *Anal. Biochem. 59,* 583.

Hanahan, D. J., Dittmer, J. C., & Warashina, Z. (1958) *J. Biol. Chem. 228,* 685.

Kleemann, W., & McConnell, H. M. (1974) *Biochim. Biophys. Acta 345,* 220.

Nicolson, G. L. (1976) *Biochim. Biophys. Acta 457,* 57.

Pagano, R. E., & Weinstein, J. N. (1978) *Annu. Rev. Biophys. Bioeng. 7,* 435.

Scandella, C. J., Devaux, P., & McConnell, H. M. (1972) *Proc. Natl. Acad. Sci. U.S.A. 69,* 2056.

Schlessinger, J., Axelrod, D., Koppel, D. Z., Webb, W. W., & Elson, E. L. (1977) *Science 195,* 307.

Shaklai, N., Yguerabide, J., & Ranney, H. M. (1977) *Biochemistry 16,* 5585.

Shimshick, E. J., & McConnell, H. M. (1973) *Biochemistry 12,* 2351.

Singleton, W. S., Gray, M. S., Brown, M. L., & White, J. L. (1965) *Am. Oil Soc. 42,* 53.

Steinberg, I. Z., & Katchalski, E. (1968) *J. Chem. Phys. 48,* 2404.

Stryer, L. (1965) *J. Mol. Biol. 13,* 482.

Stryer, L. (1978) *Annu. Rev. Biochem. 47,* 819.

Vanderkooi, J. M., Ierokomas, A., Nakamura, H., & Martonosi, A. (1977) *Biochemistry 16,* 1262.

Veatch, W., & Stryer, L. (1977) *J. Mol. Biol. 113,* 89.

Waggoner, A. S., & Stryer, L. (1970) *Proc. Natl. Acad. Sci. U.S.A. 67,* 579.

Yguerabide, J. (1972) *Methods Enzymol. 26,* 498.

Yguerabide, J., Epstein, H. F., & Stryer, L. (1970) *J. Mol. Biol. 51,* 573.

Effects of Sarcoplasmic Reticulum Ca^{2+}-ATPase on Phospholipid Bilayer Fluidity: Boundary Lipid†

B. M. Moore, B. R. Lentz,* and G. Meissner

ABSTRACT: Sarcoplasmic reticulum membrane vesicles have been isolated from rabbit skeletal muscle and delipidated to varying degrees by treatment with cholate. The structure within the hydrophobic region of cholate-free membranes has been probed by measuring the anisotropy of diphenylhexatriene fluorescence. The Ca^{2+}-ATPase activity of these samples was determined as a function of both temperature and Ca^{2+}-ATPase content. Arrhenius plots of the Ca^{2+}-ATPase activity could not be fit to straight lines over the entire range of temperature. However, Arrhenius plots of the Ca^{2+}-ATPase activity and the fluorescence-derived "microviscosity" both fit well to straight lines in the range of 20–40 °C. Both plots gave activation energies of 7–9 kcal/mol, supporting the contention that membrane fluidity is the rate-determining factor in determining Ca^{2+}-ATPase activity in the physiological temperature range. Calculations based on a precise mathematical statement of the "lipid annulus" model supported the contention that this model may offer a reasonable description of Ca^{2+}-ATPase–lipid interactions at low temperatures but is probably an oversimplified description at physiological temperatures. The dependence of Ca^{2+}-ATPase activity on membrane protein content has also been interpreted as qualitatively supporting this conclusion. Alternative explanations of the data have been explored.

Studies of the lipid dynamics within phospholipid bilayers have led to increased interest in the details of lipid–protein interactions within membrane bilayers. It is believed that intrinsic proteins inserted into or through the membrane tend to disrupt the region of the lipid bilayer in their vicinity [see Gennis and Jonas (1977) for a review]. At least two intrinsic membrane proteins (glycophorin and the acetylcholine receptor) have been reported to loosen the adjacent bilayer structure (Brûlet and McConnell, 1976; Bienvenüe et al., 1977). On the other hand, several investigators have reported results purporting to demonstrate the coexistence of normal and restricted bilayer domains within model membranes reconstituted from isolated proteins and lipids (Grant and McConnell, 1974; Faucon et al., 1976; Brown et al., 1977; Almeida and Charnock, 1977). The most convincing evidence for the existence of a restricted lipid "annulus" in the neighborhood of an intrinsic membrane protein results from studies of beef heart mitochondrial cytochrome oxidase (Jost et al., 1973a,b, 1977). Complexes of the membrane protein with

† From The Department of Biochemistry and Nutrition, University of North Carolina at Chapel Hill, Chapel Hill, North Carolina 27514. *Received June 21, 1978.* This research was supported by grants of the North Carolina Heart Association, National Science Foundation (PCM76-16761 to B.R.L.), and United States Public Health Service (AM18687 to G.M.). Part of this study was reported at the 1978 Joint Meeting of the Biophysical Society and American Physical Society in Washington, D.C.

0006-2960/78/0417-5248$01.00/0